Journal of Power Sources 228 (2013) 68–74

Contents lists available at SciVerse ScienceDirect

Journal of Power Sources

journal homepage: www.elsevier.com/locate/jpowsour

Feasibility investigation of methanol generation by CO_2 reduction using Pt/C-based membrane electrode assembly for a reversible fuel cell

Sayoko Shironita, Ko Karasuda, Masatoshi Sato, Minoru Umeda*

Department of Materials Science and Technology, Faculty of Engineering, Nagaoka University of Technology, 1603-1, Kamitomioka, Nagaoka, Niigata 940-2188, Japan

HIGHLIGHTS

- We conducted a feasibility study of the reversible reaction between methanol and CO_2.
- A detailed analysis of the CO_2 reduction was conducted on an MEA with Pt/C electrodes.
- The main product was confirmed to be methanol by GC–MS and methanol-stripping voltammetry.
- The product adsorbs too strongly on the Pt electrode to be removed.
- The CO_2 reduction occurred at a 40% Coulombic efficiency at 0.06–0.25 V vs. DHE.

ARTICLE INFO

Article history:
Received 31 August 2012
Received in revised form
8 November 2012
Accepted 24 November 2012
Available online 29 November 2012

Keywords:
Membrane electrode assembly
Carbon dioxide electroreduction
Carbon-supported platinum (Pt/C)
Polymer electrolyte fuel cell
Reversible fuel cell

ABSTRACT

In this study, we investigated the viability of a reversible fuel cell which uses methanol as the candidate liquid fuel. This fuel cell consists of methanol oxidation and its coupled carbon dioxide (CO_2) reduction reaction. The CO_2 electrode reaction using a membrane electrode assembly (MEA) with a carbon-supported platinum (Pt/C)-based anode and cathode was evaluated. First, the electrode potential of the CO_2 reduction at the MEA cathode was measured by linear sweep voltammetry. The resulting voltammograms show that the CO_2 reduction occurs within the electrode potential region of 0.06–0.4 V vs. the dynamic hydrogen electrode (DHE) in a CO_2 atmosphere. Products of the CO_2 electrode reaction were then analyzed by gas chromatograph–mass spectrometry, and a small amount of methanol was detected. Stripping voltammetry for CO and methanol was conducted, revealing that CO_2 is reduced to methanol and almost all of it strongly adsorbs onto the Pt/C cathode. Finally, the CO_2 electroreduction was shown to occur with a relatively high Coulombic efficiency of 30–50% at 0.06–0.25 V vs. DHE. Our study showed that the CO_2 reduction was able to produce methanol in an MEA with Pt/C electrodes, which may have applications in future fuel cell development.

1. Introduction

A reversible fuel cell (RFC) consisting of a polymer electrolyte fuel cell (PEFC) and a water electrolyzer is attractive as an electrical energy storage system, having shown promising results for long-term energy storage and low self-discharge [1–5]. For the hydrogen/oxygen (H_2/O_2) RFC, there have been several reports on the potential use for applications in space, in the stratosphere, and as an alternative to rechargeable batteries [6–11]. However, these fuel cells are limited by technical difficulties in the use and maintenance of H_2 at a high pressure, in terms of safety and long-term storage issues. For this reason, the use of a liquid fuel, which is free from high pressure, should be considered as a possible alternative.

The 2-propanol/acetone system is a known example of a thermally reversible fuel cell that uses liquid fuel, involving the liquid-phase dehydrogenation from 2-propanol to acetone and its reverse hydrogenation [12,13]. However, the operation of this system requires a constant supply of thermal energy, such as solar heat. The 2-propanol and acetone only act as mediators to convert heat energy to electric energy. Therefore, it is obvious that this type of fuel cell has limited application as a long-term energy storage system.

On the other hand, methanol is known to have stable storage properties in its liquid form. Thus far, the direct liquid fueling of methanol to a fuel cell has been investigated as direct methanol fuel cells (DMFCs) [14–17]. The anode and cathode reactions of the DMFCs are shown by Eqs. (1) and (2), respectively. The difference in

* Corresponding author. Tel./fax: +81 258 47 9323.
E-mail address: mumeda@vos.nagaokaut.ac.jp (M. Umeda).

0378-7753/$ – see front matter © 2012 Elsevier B.V. All rights reserved.
http://dx.doi.org/10.1016/j.jpowsour.2012.11.097

the standard electrode potentials, E^0, in these two equations shows that the theoretical electromotive force of the DMFC is 1.213 V [18], which is almost the same as the electromotive force of a PEFC (1.229 V) [19].

$$CH_3OH + H_2O \rightleftarrows CO_2 + 6H^+ + 6e^- \quad E^0 = 0.016 \text{ V} \tag{1}$$

$$3/2O_2 + 6H^+ + 6e^- \rightleftarrows 3H_2O \quad E^0 = 1.229 \text{ V} \tag{2}$$

Consequently, we will focus on the reverse reaction shown in Eq. (1). The reduction of CO_2 has been previously investigated by several researchers [20–29], in which formic acid, carbon monoxide, methane, and formaldehyde are reported as the main products. However, there has yet to be a study that has reported methanol being obtained as the main product in this process. Moreover, the reported overvoltages are very high at values greater than 1 V [20–26,28,29]. In these previous studies, CO_2 was dissolved in water when used, wherein the hydrogen evolution reaction competes with the CO_2 reduction. In this study, we used a membrane electrode assembly (MEA) to perform the CO_2 reduction at its approximate standard electrode potential [18].

The purpose of this study was to investigate the methanol generation with a major focus on the CO_2 electroreduction. For this purpose, we conducted the CO_2 reduction at a carbon-supported platinum (Pt/C) cathode of an MEA, which enables the electroreduction process to be performed with less water and a low overvoltage. We first performed the CO_2 reduction reaction at Pt/C using an MEA. The results of the initial cyclic voltammogram showed the potential range in which the reaction occurs, and the CO_2 electroreduction was then conducted accordingly under a CO_2 atmosphere. Next, the exhaust gases of this reaction were analyzed by gas chromatograph-mass spectrometry (GC–MS). Two kinds of stripping voltammetry measurements using CO and methanol were then performed to confirm the product of the reaction. Finally, the Coulombic efficiency of the CO_2 electrolysis process was electrochemically evaluated.

2. Experimental

2.1. Preparation of a single cell

The MEA (geometric electrode area: 5 cm^2) used in this study was prepared as follows [30–32]: Nafion 117 (5 × 5 cm, DuPont) was used as the polymer electrolyte membrane. The membrane was boiled in a 0.5 mol dm^{-3} H_2SO_4 solution, and then washed twice by boiling in distilled water for 1 h. Commercially available Pt/C (Pt loading: 45.7 wt%, Tanaka Kikinzoku Kogyo Co., Ltd.) powder was used for both the cathode and anode catalysts. Two to three drops of Milli-Q water were added to the Pt/C powder and mixed using a ball mill for 5 min, after which the mixture was diluted by a mixed solvent of methanol, 2-propanol, and Milli-Q water (weight ratio was 1:1:1). Next, a 5 wt% Nafion 117 solution was added to the diluted mixture so that the weight ratio was 1:6 (Nafion:Pt/C powder), and dispersed using a ball mill for one day. The obtained catalyst slurry was sprayed over a piece of water-repellent carbon paper (2.3 × 2.3 cm, TGP-H060, Toray Industries, Inc.), such that the amount of Pt was 1.0 mg cm^{-2}. Subsequently, the pretreated Nafion 117 membrane was sandwiched between two pieces of the catalyst-coated carbon paper and hot-pressed at 4.5 kN and 140 °C for 10 min. The prepared MEA was installed in a single cell (ElectroChem, Inc., E3156) having a dynamic hydrogen electrode (DHE) as the reference electrode. The DHE potential using Nafion 117 is approximately the same as that of a normal hydrogen electrode (NHE) [33,34]. The schematics of the single cell are represented in Fig. 1.

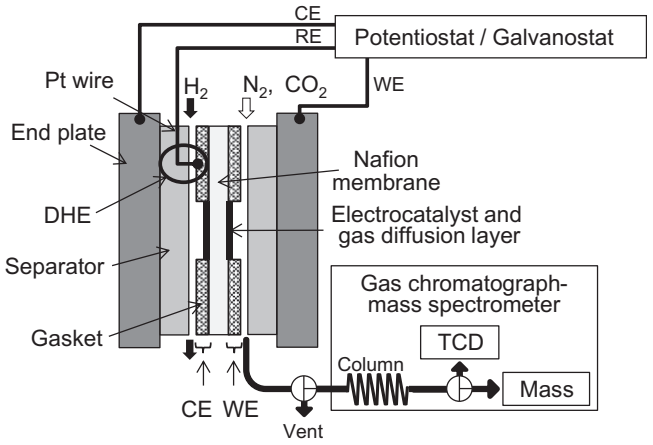

Fig. 1. Schematic of a single cell equipped with DHE reference electrode and on-line analysis system.

2.2. Electrochemical measurements

The temperature of the prepared cell was controlled at 40 °C. Humidified N_2 (purity: 99.999%) and humidified H_2 (purity: 99.999%) were supplied to the working and counter electrodes, respectively, at the flow rate of 50 cm^3 min^{-1} by a PEFC power generation unit (HPE-1000, FC Development Co., Ltd.) [35]. Under these conditions, the electrode potential was swept at the rate of 50 mV s^{-1} and the potential range of the observed voltammogram was stabilized at 0.06–1.40 V vs. DHE. Next, the supplied gas for the working electrode was changed from humidified N_2 to humidified CO_2 (purity: 99.995%), and the cyclic voltammogram was then measured at the rate of 10 mV s^{-1} in the potential range of 0.06–1.40 V vs. DHE. All gases in this study were fully humidified at all the subsequent temperatures for the measurements.

2.3. Analyses of products

To analyze the products of the reaction, the cell cathode was operated at 0.060 V vs. DHE at 26, 60, 80 and 90 °C by supplying humidified CO_2 to the working electrode and humidified H_2 to the counter electrode. The exhaust gas was directly analyzed by a gas chromatograph-mass spectrometer (GC–MS: GCMS-QP2010 Ultra, Shimadzu) equipped with the CP Pora PLOT U capillary column and thermal conductivity detector (TCD-2010 Plus) as shown in Fig. 1. Column temperature was set at 40 °C and held for 6 min, then programmed up to 180 °C at 15 °C min^{-1}. Injection, interface and ion source temperature were set at 100 °C, 190 °C, and 200 °C, respectively. Helium was used as carrier gas at a flow rate of 3.62 cm^3 min^{-1}. The mass spectrometer was operated in an electron impact ionization mode at an ionization energy of 70 eV. The sensitivity of mass detector was −0.2 and −0.3 kV. Full scan data were obtained with a mass range of m/z 2–100.

The CO-stripping voltammetry was performed as follows: The working electrode potential was fixed at 0.10 V vs. DHE, and humidified CO at 10 cm^3 min^{-1} and humidified H_2 at 50 cm^3 min^{-1} were supplied to the working and counter electrodes, respectively, for 10 min. Thereafter, humidified N_2 was supplied to the working electrode for 1 h at 50 cm^3 min^{-1}, while the electrode potential was maintained at 0.10 V vs. DHE. The 2-cycle voltammogram was obtained between the ranges of 0.06–1.30 V vs. DHE with the sweep rate of 10 mV s^{-1}.

The methanol-stripping voltammetry was performed as follows: Similar to the CO-stripping measurement, the working electrode potential was fixed at 0.10 V vs. DHE; and N_2 gas bubbled

into a bottle of liquid methanol at 50 cm^3 min^{-1} (Purity: 99.95%, Wako) and humidified H_2 at 50 cm^3 min^{-1} were supplied to the working and counter electrodes, respectively, for 10 min. Thereafter, 50 cm^3 min^{-1} humidified N_2 was supplied to the working electrode for 1 h, while the electrode potential was maintained at 0.10 V vs. DHE. The voltammogram was then measured using the same procedure for the CO-stripping measurement.

3. Results and discussion

3.1. Cyclic voltammograms under a CO_2 atmosphere

To investigate the CO_2 reduction reaction, a cyclic voltammogram was measured at the working electrode using a single cell equipped with a reference electrode (DHE). The results are shown in Fig. 2, represented by the solid line. For comparison, the result under a N_2 atmosphere is presented in the same figure as the dotted line. Under the N_2 atmosphere, a typical cyclic voltammogram of Pt was observed, representing characteristics such as the H-adsorption/desorption at 0.06–0.30 V vs. DHE, the formation of an oxide layer on the Pt surface at 0.80–1.40 V vs. DHE, and the reduction of the Pt oxide layer at around 0.70 V vs. DHE [36].

In the CO_2 atmosphere, three characteristic peaks were observed in Fig. 2, designated as Region 1, Region 2, and Region 3. In Region 1, the reduction current under the CO_2 atmosphere was observed to be as high as that under the N_2 atmosphere. In Region 2, the H-desorption region, the oxidation current under the CO_2 atmosphere is lower than that under the N_2 atmosphere. This implies that the desorption amount of adsorbed H on the cathode surface under the CO_2 atmosphere is lower than that under the N_2 one. However, this result was inconsistent with the observation in Region 1. In Region 3, a new current peak was observed under the CO_2 atmosphere, whereas there is no peak under the N_2 atmosphere. Based on these results, it is deduced that the CO_2 reduction occurs in Region 1, which competes with the H-adsorption reaction, and the CO_2 reduction product or intermediate is reoxidized in Region 3.

3.2. Electrochemical quantitative analysis of CO_2 reduction

According to the aforementioned deduction, we can assume that the oxidation peak in Region 3 of Fig. 2 indicates the reoxidization of the CO_2 reductant. Based on this assumption, a linear sweep voltammogram was then measured by changing the initial holding potential. The initial holding potential was gradually changed from 0.06 to 0.40 V vs. DHE for 5 min under humidified CO_2 flowing at 50 cm^3 min^{-1}. The electrode potential was then swept in a positive direction to obtain the linear sweep voltammogram (0.06–1.40 V vs. DHE, 10 mV s^{-1}). These results are represented in Fig. 3, which show that the reoxidized peak of the CO_2 reductant decreases when the holding potential is more than 0.20 V vs. DHE.

The relationship between the coulomb charge of the peak in Region 3 versus the initial holding potential is plotted in Fig. 4. The magnitude of this charge is observed to decrease with a shift in the holding potential from 0.20 V vs. DHE in the anodic direction, while it is almost the same at 0.20–0.05 V vs. DHE. This result suggests that the amount of adsorbed materials is saturated by the 5-min electrolysis at 0.06–0.20 V vs. DHE.

3.3. GC–MS analysis

We analyzed reaction products of the CO_2 reduction at the Pt/C electrocatalyst in the single cell using the on-line GC–MS. The CO_2 electrolysis was conducted for 30 min at 0.060 V vs. DHE at 26, 60, 80 and 90 °C, and the exhausted gas was directly introduced to the GC–MS as shown in Fig. 1. A total ion chromatogram (TIC) and the controlled column temperature are shown in Fig. 5a. The column temperature is elevated as shown in upper the graph of Fig. 5a. In the bottom graph of Fig. 5a, observed peaks at around 6 and 16 min are identified to be CO_2 and H_2O, respectively. These peaks are too large to find other peaks. Then, we increased the sensitivity of mass detector from −0.3 kV to −0.2 kV; while, the CO_2 and H_2O were introduced to the TCD unit during their retention time. The obtained TIC results are shown in Fig. 5b. From this graph, a small peak is observed around 17.3 min at the cell temperature of 80 and 90 °C.

Then, the peaks were qualitatively analyzed by mass spectra. The mass spectrum at 17.3 min retention time is shown in Fig. 5c (bottom). For identifying, a library datum of methanol is also shown in upper graph of Fig. 5c. From these graphs, the main peaks of $m/z = 29$, 31, and 32 well agree. Consequently, the detected small peak is attributed to the generated methanol which is exhausted from the cell.

Next, to assess the temperature dependency of methanol detection, the ion chromatograms of $m/z = 29$ and 31 are shown in Fig. 5d. For each mass numbers, the peak is observed at 80 and 90 °C. The elevated temperature makes the adsorbed methanol on the Pt/C easier to be exhausted from the cell. Any other peaks based on CO, methane, and ethanol were not found in the exhaust gas.

3.4. CO- and methanol-stripping voltammograms

Based on these results, stripping voltammetry measurements were conducted to confirm the CO_2 reduction product. According to

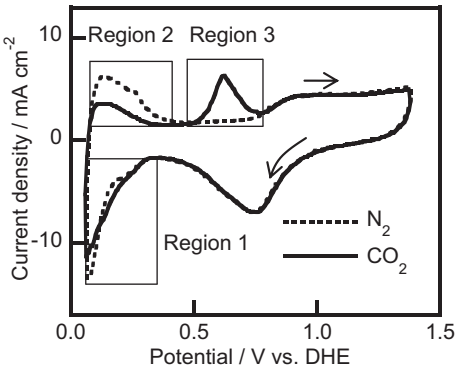

Fig. 2. Cyclic voltammograms obtained under N_2 (dotted line) and CO_2 (solid line) atmospheres for the working and counter electrodes, respectively. Cell temperature: 40 °C, scan rate: 10 mV s^{-1}.

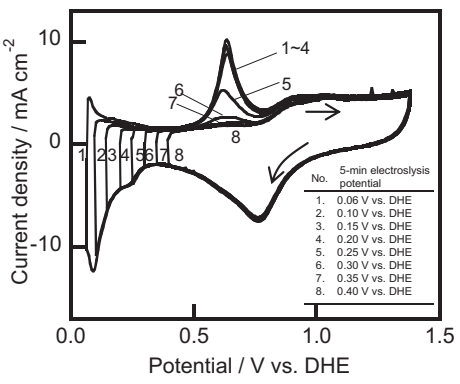

Fig. 3. Cyclic voltammograms obtained in CO_2 atmosphere by changing the 5-min electrolysis potential. Cell temperature: 40 °C, scan rate: 10 mV s^{-1}.

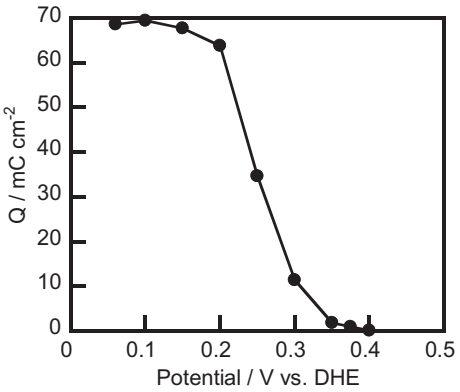

Fig. 4. Five-min electrolysis potential dependence of coulomb charges (Q) for the peak observed between 0.5 and 0.85 V vs. DHE in Fig. 3. Plots are taken from Fig. 3.

previous reports, CO is generated as a product of the CO_2 electroreduction [21–26,28]. In this experiment using Pt/C, there is a possibility that CO strongly adsorbs on the Pt and is not detected by the gas chromatograph or mass spectrometer.

Along with this consideration, the CO-stripping voltammogram was measured. The result is shown in Fig. 6. The solid line and the dotted line in the figure indicate the first and second cycles, respectively. It was found that CO is completely desorbed by oxidation during the first cycle, as the voltammogram of the second cycle was almost identical in shape to that obtained under the N_2 atmosphere (see Fig. 2). This result shows that the CO oxidation began from 0.60 V vs. DHE on the Pt/C, and two oxidation peaks are observed at 0.65 and 0.80 V vs. DHE. Because the types of CO adsorptions on Pt surfaces are different, two oxidation peaks were observed [37,38]. For this reason, it seems that the CO-stripping voltammogram does not coincide with the result of Fig. 3.

The results of the methanol stripping are shown in Fig. 7 in which the solid and dotted lines indicate the first and second cycles, respectively. The second cycle in Fig. 7 indicates that methanol is completely oxidized. The first cycle shows an onset potential of 0.4 V vs. DHE, and the peak of the methanol oxidation is at 0.60 V vs. DHE [39]. This is almost identical to the observations in Fig. 3, in which the reoxidation onset potential is at 0.45 V vs. DHE and the peak is located at approximately 0.60 V vs. DHE. These results together with the chromatography result clearly point out that the reoxidation peak obtained from the CO_2 reduction is attributed to

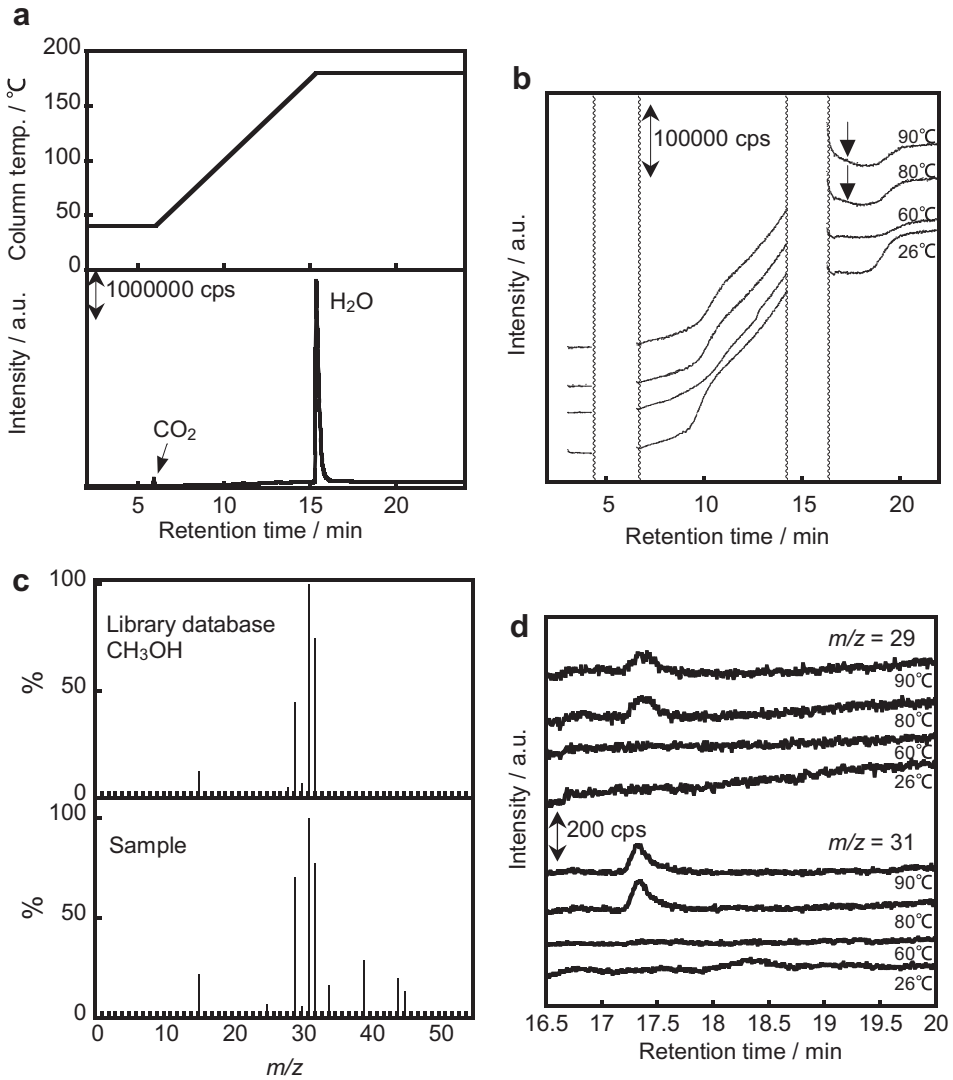

Fig. 5. Results of on-line GC–MS measurement, (a) Time stream of column temperature and total ion chromatograph at −0.3 kV of mass sensitivity, (b) total ion chromatographs at 26, 60, 80 and 90 °C at −0.2 kV of mass sensitivity, (c) a methanol spectrum from library database (upper) and sample spectrum at 80 °C (bottom), and (d) temperature dependency of $m/z = 29$ and 31 ion chromatographs.

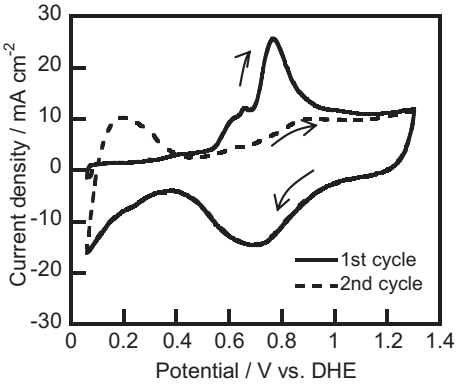

Fig. 6. CO-stripping voltammograms under N_2 atmosphere. Cell temperature: 40 °C, scan rate: 10 mV s^{-1}.

the methanol oxidation reaction, and the methanol generated is known to be strongly adsorbed on the Pt surface.

3.5. Analysis of the CO_2 reduction potential

Based on the results from the last section, methanol was deduced to be the main product of the process. Based on Figs. 3 and 4, the CO_2 reduction was shown to occur at 0.06–0.4 V vs. DHE. These potentials are more positive than 0.016 V vs. NHE, which is the standard electrode potential of Eq. (1). In general, no current is observed in the case of the coupled reversible reactions at the standard electrode potential because of the balanced anodic and cathodic currents. When we look at the reduction reaction, it proceeds even when the potential is more positive than the standard electrode potential [40]. However, this small reduction current is unable to be observed due to the relatively large coupled oxidation current.

The methanol oxidation reaction (MOR), which is a coupled reaction of the CO_2 reduction, accompanies the formation of CO and other intermediates that strongly adsorb on the surface of the Pt/C electrode [41]. For this reason, the onset potential of the MOR shifts in the positive direction and is observed at 0.4 V vs. NHE as shown in Fig. 7. As a result of this anodic potential shift of the coupled MOR, it could be considered that the CO_2 reduction is observed at 0.06–0.4 V vs. DHE, as seen in Fig. 4, which is a substantially more positive potential than the standard electrode potential of 0.016 V vs. NHE.

It should be noted that the CO_2 reduction process is performed on the Pt/C cathode of the MEA in this experiment. Under these conditions, the hydrogen evolution reaction as a competition reaction can be suppressed because only a small amount of water is present. Therefore, the CO_2 reduction significantly occurred at the Pt/C of the MEA.

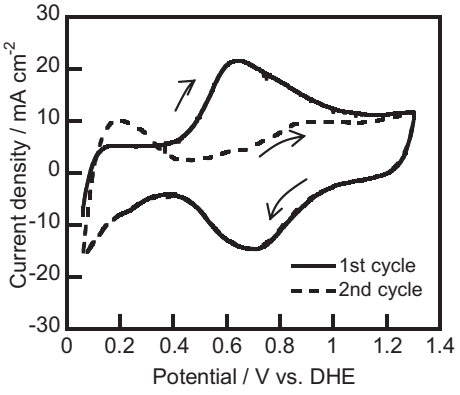

Fig. 7. Methanol-stripping voltammograms under N_2 atmosphere. Cell temperature: 40 °C, scan rate: 10 mV s^{-1}.

3.6. Coulombic efficiency of the CO_2 reduction reaction

The reduction reaction observed at Region 1 in Fig. 2 was thought to be the competitive reactions of (i) the CO_2 reduction and (ii) the H adsorption on Pt. A comparison of the Coulombic efficiency of both reactions was carried out by calculating the ratios from the H adsorption (E_H) and the CO_2 reductant (E_R) using the coulomb charges of each region as shown in Fig. 3. The ratios are calculated using Eqs. (3) and (4).

$$E_H = Q_{des}(H)/Q_{ads} \times 100 \quad (3)$$

$$E_R = Q_{des}(Red)/Q_{ads} \times 100 \quad (4)$$

where $Q_{des}(H)$ represents the charges caused by the H desorption in Region 2, $Q_{des}(Red)$ represents the charges caused by the reoxidation of the CO_2 reductant in Region 3, and Q_{ads} represents the total reduction charges observed in Region 1.

For this evaluation, a cyclic voltammetry measurement was conducted only by changing the cathodic potential limit of the voltammogram shown in Fig. 2. The Coulombic efficiencies of E_H and E_R were calculated using Eqs. (3) and (4), respectively, and plotted versus the lower potential limit of the cyclic voltammetry in Fig. 8. In this figure, the Coulombic efficiencies are indicated by an open circle (E_H) and a closed circle (E_R). The results show that the Coulombic efficiency of the CO_2 reduction ranged between 30 and 50% at 0.06–0.25 V vs. DHE, and that this value is not dependent on the lower potential limit of the cyclic voltammetry.

Next, the yield methanol in the exhausted gas was calculated using the data of Fig. 5. Table 1 shows the calculated Coulombic efficiency using current charges and detected methanol amount. By comparing the results of Table 1 and Fig. 8, the Coulombic efficiency of methanol oxidation obtained by the CV data is about 40%, whereas that detected in the exhausted gas is infinitesimal. Therefore, methanol is produced from CO_2 with high efficiency, but almost all methanol adsorbs on the Pt/C electrocatalyst surface which is scarcely exhausted from the cell.

Moreover, chronoamperometry was conducted at 0.051 V vs. DHE by supplying the humidified CO_2 and humidified H_2 to the working and counter electrodes, respectively, for 1 h. The result is shown in Fig. 9, which demonstrates the continuous reduction of

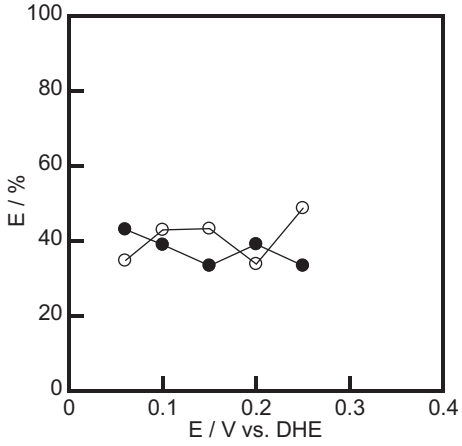

Fig. 8. The Coulombic efficiency of a desorbed H (closed circle) and generated CO_2 reductant (open circle) as a function of the lower potential limit of the cyclic voltammetry.

Table 1
Coulombic efficiency of the yielded methanol out of the cell. Data are taken from Fig. 5.

Temperature/°C	Coulombic efficiency/%
26	N.D.
60	N.D.
80	3.17×10^{-2}
90	3.05×10^{-2}

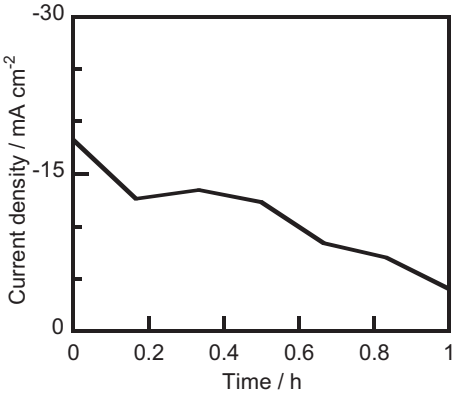

Fig. 9. Time dependence of CO_2 electrolysis current for 1 h. Cell temperature: 40 °C, working potential: 0.051 V vs. DHE.

CO_2. However, the magnitude of the current was observed to decrease with the increasing electrolysis time. The results of the methanol-stripping voltammograms, as mentioned earlier, show that methanol strongly adsorbs on the Pt surface. The results observed in Fig. 9 can therefore be explained by the increasing accumulation of methanol on the Pt surface, which consequently results in a decrease in the number of active sites on the Pt electrode.

In Fig. 8, the CO_2 electrolysis was conducted by cyclic voltammetry, and the results show that the Coulombic efficiency of the CO_2 reduction is approximately 40% in the potential range of 0.06–0.25 V vs. DHE. However, as shown in Fig. 9, the reduction current decreased with an increase in the electrolysis time. The difference observed between these two results can be explained by the fact that the electrolysis was conducted for a short period of time in the first case (Fig. 8) and for a longer period of time in the second one (Fig. 9). At present, it is possible to detect only a small amount of methanol in the exhaust gas, but our analysis showed distinct evidence that the CO_2 reduction proceeds with a high Coulombic efficiency of 40% in the cell. Accordingly, it is likely that almost all of the CO_2 reductant is strongly adsorbed on the Pt cathode. If these adsorbates can be efficiently removed from the cell, we can expect the CO_2 reduction process to continuously occur without any decrease in the reduction current by catalyst poisoning.

In the near future, we plan to develop the electrocatalyst which can easily release the adsorbed methanol. This enables to realize a reversible fuel cell by utilizing the methanol production reaction.

4. Conclusions

In this study, we have performed the CO_2 reduction using an MEA with a Pt/C-based electrode under a CO_2 gas atmosphere. A summary of the results is as follows:

(1) Cyclic voltammograms were measured under a CO_2 atmosphere, and a new oxidation current peak was observed at approximately 0.6 V vs. DHE. This peak was considered to be the reoxidation peak of the CO_2 reduction.
(2) By varying the lower potential limit of the cyclic voltammetry, we observed that the magnitude of the reoxidized peaks was dependent on this potential. The CO_2 reduction was observed to occur at 0.06–0.4 V vs. DHE.
(3) Exhaust gas from the CO_2 electroreduction process was analyzed by GC–MS, which showed the presence of a small amount of methanol.
(4) A methanol-stripping voltammogram confirmed that the main product of the CO_2 electroreduction is methanol. It was deduced that almost all the methanol produced by the CO_2 reduction is adsorbed on the Pt electrode.
(5) Coulombic efficiency of the CO_2 reduction was evaluated by a cyclic voltammetry measurement, and was found to occur at the high Coulombic efficiency of 40% at 0.06–0.25 V vs. DHE. However, for a 1 h operation, it was speculated that the CO_2 reduction product of the methanol accumulates on the active site of the Pt/C electrocatalyst, thereby reducing the reduction current with time.

Acknowledgements

A part of this work was supported by MEXT/JSPS KAKENHI (gs1) Grant Numbers (24350091 and 24651073).

References

[1] A.B. LaConti, L. Swette, in: W. Vielstich, A. Lamm, H.A. Gasteiger (Eds.), Handbook of fuel cells, vol. 4, John Wiley and Sons Ltd, England, 2003, pp. 745–761.
[2] T. Ioroi, T. Oku, K. Yasuda, N. Kumagai, Y. Miyazaki, Journal of Power Sources 124 (2003) 385–389.
[3] C.M. Hwang, M. Ishida, H. Ito, T. Maeda, A. Nakano, A. Kato, T. Yoshida, Journal of Power Sources 202 (2012) 108–113.
[4] S.A. Grigoriev, P. Millet, V.I. Porembsky, V.N. Fateev, International Journal of Hydrogen Energy 36 (2011) 4164–4168.
[5] P. Millet, R. Ngameni, S.A. Grigoriev, V.N. Fateev, International Journal of Hydrogen Energy 36 (2011) 4156–4163.
[6] C.C. Badcock, Aerospace America 22 (1984) 68–72.
[7] D.W. Sheibley, NASA Conference Publications (1984) 23–38.
[8] G.M. Reppucci, A.A. Sorensen, Intersociety Energy Conversion Engineering Conference 20 (1985) 66–73.
[9] A.J. Appleby, Journal of Power Sources 22 (1988) 377–385.
[10] Y. Sone, Journal of Power Sources 196 (2011) 9076–9080.
[11] J. Giner, A. LaConti, in: V. Barsukov, F. Beck (Eds.), New Promising Electrochemical Systems for Rechargeable Batteries, Kluwer Academic Publishers, Dordrecht, 1996, pp. 215–232.
[12] Y. Ando, T. Tanaka, T. Doi, T. Takashima, Energy Conversion and Management 42 (2001) 1807–1816.
[13] Y. Ando, Y. Aoyama, T. Sasaki, Y. Saito, H. Hatori, T. Tanaka, Bulletin of the Chemical Society of Japan 77 (2004) 1855–1859.
[14] R. Dillon, S. Srinivasan, A.S. Aricò, V. Antonucci, in: N. Brandon, D. Thompsett (Eds.), Fuel Cells Compendium, Elsevier, Amsterdam, Netherlands, 2005, pp. 167–187.
[15] D.C. Dunwoody, H. Chung, L. Haverhals, J. Leddy, in: S. Minteer (Ed.), Alcoholic Fuels, Taylor & Francis, FL, 2006, pp. 155–189.
[16] S. Prakash, W.E. Mustain, P.A. Kohl, in: T.S. Zhao (Ed.), Micro Fuel Cells: Principles and Applications, Elsevier, Amsterdam, Netherlands, 2009, pp. 1–50.
[17] J. Kawaji, S. Suzuki, Y. Takamori, M. Morishima, Electrochimica Acta 55 (2010) 8018–8022.
[18] C. Lamy, E.M. Belgsir, J.-M. Léger, Journal of Applied Electrochemistry 31 (2001) 799–809.
[19] W. Vielstich, in: W. Vielstich, A. Lamm, H.A. Gasteiger (Eds.), Handbook of Fuel Cells, vol. 1, John Wiley and Sons Ltd, England, 2003, pp. 26–30.
[20] P.G. Russell, N. Kovac, S. Srinivasan, M. Steinberg, Journal of Electrochemical Society 124 (1977) 1329–1338.
[21] M. Watanabe, M. Shibata, A. Katoh, Journal of Electroanalytical Chemistry 305 (1991) 319–328.
[22] G. Kyriacou, A. Anagnostopoulos, Journal of Electroanalytical Chemistry 322 (1992) 233–246.
[23] Y. Hori, H. Wakebe, T. Tsukamoto, O. Koga, Electrochimica Acta 39 (1994) 1833–1839.
[24] T. Yamamoto, D.A. Tryk, A. Fujishima, H. Ohta, Electrochimica Acta 47 (2002) 3327–3334.

[25] Y. Hori, I. Takahashi, O. Koga, N. Hoshi, Journal of Physical Chemistry B 106 (2002) 15–17.
[26] I. Takahashi, O. Koga, N. Hoshi, Y. Hori, Journal of Electroanalytical Chemistry 533 (2002) 135–143.
[27] J. Liu, H. Yan, K. Wang, E. Wang, Journal of Applied Electrochemistry 34 (2004) 757–762.
[28] M. Gattrell, N. Gupta, A. Co, Energy Conversion and Management 48 (2007) 1255–1265.
[29] J. Christophe, T. Doneux, C. Buess-Herman, Electrocatalysis 3 (2012) 139–146.
[30] M. Inoue, T. Iwasaki, K. Sayama, M. Umeda, Journal of Power Sources 195 (2010) 5986–5989.
[31] M. Umeda, K. Sayama, M. Inoue, Journal of Renewable and Sustainable Energy 3 (2011) 043107.
[32] M. Inoue, T. Iwasaki, M. Umeda, Electrochemistry 79 (2011) 329–333.
[33] B. Seger, K. Vinodgopal, P.V. Kamat, Langmuir 23 (2007) 5471–5476.
[34] M. Umeda, K. Sayama, T. Maruta, M. Inoue, Ionics (2012). http://dx.doi.org/10.1007/s11581-012-0791-z.
[35] M. Umeda, S. Kawaguchi, I. Uchida, Japan Journal of Applied Physics 45 (2006) 6049–6054.
[36] B.E. Conway, H. Angerstein-Kozlowska, W.B.A. Sharp, E.E. Criddle, Analytical Chemistry 45 (1973) 1331–1336.
[37] N.M. Marković, C.A. Lucas, B.N. Grgur, P.N. Ross, Journal of Physical Chemistry B 103 (1999) 9616–9623.
[38] N.M. Marković, C.A. Lucas, A. Rodes, V. Stamenković, P.N. Ross, Surface Science 499 (2002) L149–L158.
[39] V. Baglio, A. Stassi, A. Di Blasi, C. D'Urso, V. Antonucci, A.S. Aricò, Electrochimica Acta 53 (2007) 1360–1364.
[40] C.H. Hamann, A. Hamnett, W. Vielstich, in: Electrochemistry, second ed., WILEY-VCH Verlag GmbH & Co. KGaA, Weinheim, 2007, pp. pp.166–169.
[41] A. Hamnett, in: W. Vielstich, A. Lamm, H.A. Gasteiger (Eds.), Handbook of Fuel Cells, vol. 1, John Wiley and Sons Ltd, England, 2003, pp. 305–322.